

Novel PID Controller on Battery Energy Storage Systems for Frequency Dynamics Enhancement

Muhammad Abdillah¹, Tirta Jayadiharja², R Harry Arjadi³, Herlambang Setiadi^{4*}, Ramon Zamora⁵, and Yusrizal Afif⁶

^{1,2} Department of Electrical Engineering, Universitas Pertamina, Jakarta, Indonesia

³ Pusat Penelitian Teknologi Pengujian, Lembaga Ilmu Pengetahuan Indonesia, Tangerang Selatan, Indonesia

^{4,6} Faculty of Advanced Technology and Multidiscipline, Universitas Airlangga, Surabaya, Indonesia

⁵ Department of Electrical Engineering, Auckland University of Technology, Auckland, New Zealand

Email: ¹ m.abdillah@universitaspertamina.ac.id, ² tirtajayadiharja@gmail.com, ³ r.harry.arjadi@brin.go.id,

⁴ h.setiadi@ftmm.unair.ac.id, ⁵ ramon.zamora@aut.ac.nz, ⁶ yusrizal@ftmm.unair.ac.id

*Corresponding Author

Abstract—Frequency dynamics is one of the important aspects of power system stability. From the frequency dynamics, the operator could plan how is the reliability of the electricity. The frequency can be maintained by controlling the balance between load demand and generation. To maintain the balance of the generation, the governor is playing an important role to increase the speed of the turbine and enhance the generating capacity of the generator (ramp-up). However, as the speed of the governor is slower than the increasing load demand, in the sub-transient area, the frequency may experience higher overshoot. Hence, it is important to add additional devices such as battery energy storage systems to enhance the frequency dynamics response in the sub-transient area. One of the important parts of storage is the controller. The controller must make sure the storage charges and discharge energy are in the sub-transient area. Hence PID controller can be the solution to make the storage operate optimally. This paper proposed a novel PID controller on battery energy storage systems (BESS) to enhance the dynamics performance of frequencies. The five-area power system is used as the test system to investigate the efficacy of the proposed novel idea. Time domain simulation is investigated to see the improvement of the frequency dynamics response. From the simulation results, it is found that adding a PID controller on BESS could enhance the BESS response and result in frequency dynamics response improvement.

Keywords—Battery Energy Storage System; Clean Energy Technology; Energy Governance; Multi-area Automatic Generation Control; Proportional Integral Derivative.

I. INTRODUCTION

In these modern times, the demand deviates from its normal state by an unpredictable small amount [1]. Therefore, the system may suffer from nominal frequency deviations, which can produce undesired effects [2]. Thermal Generating Unit (TGU) needs to continuously supply electricity with increasing demand [3]. Automatic Generation Control (AGC) has the role to maintain oscillation frequency and tie-line power in unpredictable load changes [4]. The AGC controller parameter has a significant influence on the control performance of Area Control Error (ACE), which measures the balance of generation with electricity demand, and contract compliance between control areas [5]. It is called secondary control and requires each control area to fulfill its demand [6]. As a result, it can maintain the nominal frequency in the system [7]. The main aim of this paper is to help to solve

the frequency problem on multi-area and five-area AGC interconnects TGU non-reheat systems [8].

The power system is tasked with maintaining a balance between power demand and power generation so that high-quality and reliable electricity is available to users [9]. To do that integral controller, PI control, and PID controller are used in the AGC. The application of integral control for AGC is reported in [10]. In [10], renewable energy integration is considered. In addition, the integral controller is optimized using the auction-based algorithm. The research effort in [11], proposed a PID controller as the AGC controller. It is reported that the PID controller is giving satisfactory control for balancing the demand and production. The application of fuzzy-PID to maintaining the balance between demand and production is reported in [6]. In [6], the hydro-thermal power system is considered as the source. In addition, high voltage direct current (HVDC) lines are also considered in the system. From the simulation results, it is observed that the fuzzy-PID can be used to control the hydro-thermal power plant governor for maintaining the balance between the power and the demand. The application of the 3DOF-POD controller for frequency enhancements is reported in [12]. The renewable energy power plant is considered in the system. From the simulation results, it is noticeable that the proposed method can help the system to maintain the frequency response. However, if the interconnected system is more than two areas, controlling only the governor to enhance the frequency dynamics response is out of date. Hence, it is important to add additional devices that can store and release electricity power in a short time [13], [14].

Battery energy storage systems (BESS) can be used as additional devices that can use to enhance the frequency dynamic performance [15]. BESS can use to store and releasing energy in a short period [16]. The application of BESS to help AGC for enhancing the frequency response of the power system is reported in [17]. From the simulation results, it is noticeable that BESS can help AGC to enhance the frequency performance by storing and releasing energy in a short period. The application of BESS for frequency regulation in islanded power systems is reported in [18]. From the simulation results, it is noticeable that BESS can be used to regulate the frequency. It is found that the frequency has less overshoot and faster settling time compared with the



system that only uses AGC. Asian Development Bank (ADB) publishes a handbook regarding the application of BESS [19]. From the book, it is reported that BESS can solve numerous problems associated with the integration of energy in large-scale grids. However, very scant attention has been made to developing the controller of BESS for enhancing the frequency dynamic response of power systems [20]. Hence, it is important to contribute to this area.

PID controller is one the most practical controller in engineering applications [21]. The application of PID controller for DC-DC converter controller is reported in [22]. From the results, it is noticeable that PID could provide a signal controller to the DC-DC converter. The research effort in [23], tries to utilize the PID controller as the DC motor controller. It is found that the DC motor speed has less overshoot and faster settling time when using the PID controller as the controller. The application of the PID controller as the controller of the flywheel energy storage system (FESS) is reported in [24]. From the simulation, it is proven that FESS with PID could provide better active power to the grid. In addition, many industries use PID controllers due to their simplicity and easy-to-understand structure [25]. Hence it is important, to add a PID controller as an additional controller of BESS.

This paper proposed a novel method of adding a PID controller as an additional controller of BESS. Five areas of the interconnected power system are used as the test system of the paper. The rest of the paper is organized as follows: Section 2 describes the fundamental theory of the paper. Results and Discussion are described in Section 3. Section 4 highlighted the contribution and conclusion of the paper.

II. FUNDAMENTAL THEORY

In the electric power system, the frequency is a variable that is constantly changing because it is influenced by the generator and load. To stabilize the power system operation, the frequency is always maintained according to the limit permitted. The standard operation of different frequencies under normal and abnormal conditions has been carried out by different system operators are shown in Table I.

TABLE I. FREQUENCY QUALITY PARAMETERS IN THE SYNCHRONIC AREA OF ALSO-E

	CE	GB	IRE	NE
<i>Nominal Frequency</i>	50 Hz	50 Hz	50 Hz	50 Hz
<i>Standard Frequency Range</i>	±50 mHz	±200 mHz	±200 mHz	±100 mHz
<i>Maximum Instantaneous Frequency Deviation</i>	±800 mHz	±800 mHz	±1000 mHz	±1000 mHz
<i>Maximum Steady State Frequency Deviation</i>	±200 mHz	±500 mHz	±500 mHz	±500 mHz
<i>Time to Recover Frequency</i>	15 min	1 min	1 min	15 min

The operating frequency standards set by the European Network of Transmission System Operators for Electricity (ENTSO-E) are shown in Table I. There are four synchronous regions in Europe. The territory of Great Britain (GB) is forming its synchronous area. In the Continental Europe (CE) region are the areas of Austria, Belgium, Bosnia, Bulgaria, Croatia, Czech Republic, France, Germany, Greece, Herzegovina, Hungary, Luxembourg, Italy, Macedonia, Netherlands, Montenegro, Poland, Portugal, Romania, Serbia,

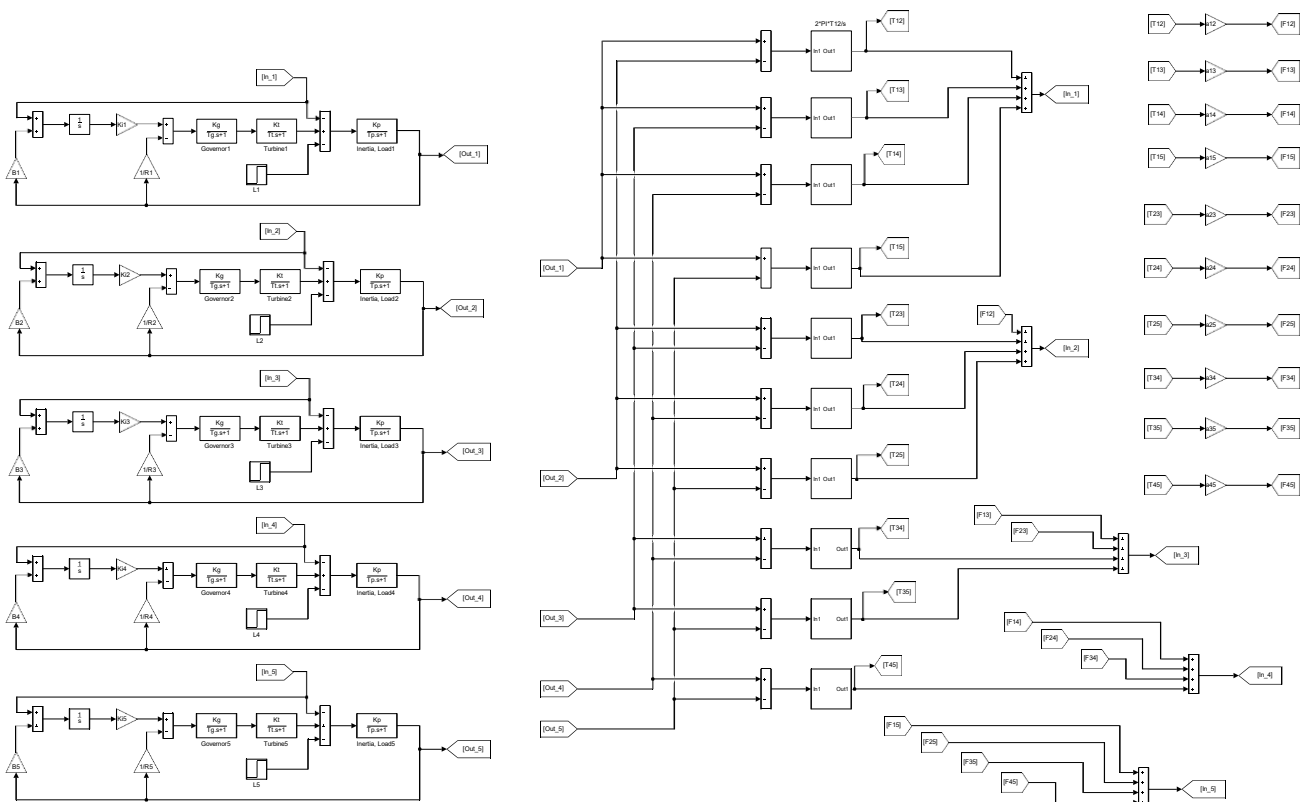


Fig. 1. Interconnection Model of Five Areas of Non-Reheat Thermal Generation System

Slovakia, Slovenia, Spain, Switzerland, and western Denmark. The Inter-Nordic System (NE) is a transmission network in eastern Denmark, Finland, Norway, and Sweden. The All-Island Irish System (IRE) is the area of the Republic of Ireland and does not include Northern Ireland.

A. Automatic Generation Control

The power output generated by the generator in a multi-area power generation system interconnected via a power exchange (tie-line) must be of high quality [26]. These characteristics include a stable frequency and output voltage. A power generation system must be able to respond to load changes by releasing the necessary power [27]. A controller system is required to maintain the stability of the system output, which is commonly referred to as AGC, to have a stable output of power, frequency, and voltage. AGC works by adjusting the valve opening on the turbine to compensate for changes in power so that the power, frequency, and voltage remain stable [28].

In an electric power system, the generator will release two types of power: active power and reactive power. The active power on the generator causes the frequency to rise and fall in response to changes in the active power released. To stabilize the frequency oscillation, a controller system that can adjust the generator's output frequency is required [29]. This control system is commonly referred to as Load Frequency Control (LFC) [30]. Changes in the active power removed from the generator are influenced by the rotor angle (δ) and the frequency value (f), while changes in the reactive power in the generator are influenced by the voltage magnitude [31].

A change in the rotor angle $\Delta\delta$ will cause a change in the value of the tie-line power and the output frequency. To correct this, the rotor angle error signal must be corrected [32]. The generator's output frequency and tie-line power will be used as input signals to the governor's valve controller [33]. The output signal at the valve will be an input to the prime mover to increase or decrease torque depending on the magnitude value of the input signal. Changes in the output value of the generator (ΔP_G) are affected by the prime mover and this condition will change the value of frequency Δf and tie-line power ΔP_{tie} [34].

LFC is designed based on the rotor angle setting on the generator. Changes in the rotor angle will be corrected so that the system frequency will be stable. The frequency deviation signal Δf and ΔP_{tie} is amplified and converted into an active signal which will be sent to the prime mover to increase torque [35].

B. Inertia Representation

To control the system frequency in a synchronous generator, the active power, and the resulting kinetic energy function must be controlled [36]. The rotor's rotating mass generates inertia power measured in joules-seconds ($J\cdot s$) or watt-seconds squared ($W\cdot s^2$) [37]. This inertia power is used to compensate for a disturbance during the first 1-5 seconds of operation or when the primary and secondary controls are not activated [38]. Based on the swing equation, the inertial response of a synchronous machine can be written as follows, as described in (1) [31].

$$J_S \frac{d\omega}{dt} = T_m - T_e = \frac{P_m}{\omega} - \frac{P_e}{\omega} \quad (1)$$

Where J_S , ω , T_m , T_e , P_m , P_e , is the moment of inertia, rotor speed, mechanical torque, electrical torque, mechanical power, and electrical power. (2) and (3) [39] describe the mathematical representation of inertia (3). Where S is the synchronous generator's power rating output [40].

$$H = \frac{E_{kinetik}}{S} \quad (2)$$

$$E_{kinetik} = \frac{1}{2} J_S \omega^2 \quad (3)$$

When the system is made up of several interconnected generators, the total inertia constant is the ratio of the kinetic energy of each generator added together [41]. Furthermore, the system output power rating influences the inertia constant. As a result, referring to the total inertia can be written using (4) [42].

$$H = \frac{\sum_i (H_i S_{SGi})}{S_{PS}} \quad (4)$$

Where the system's minimum inertia can be used to solve two major dynamic problems. The first issue is lowering the rate of change of frequency ($RoCof$) after the perturbation appears. The second issue is to dampen frequency overshoot and limit frequency nadir when there is a disturbance in the system. $RoCof$ is the deferential frequency used to calculate the system's inertia response. The system's $RoCof$ value should be limited to ± 1 Hz/s. $RoCof$'s mathematical representation can be described using (5) [43]. Where f_0 is the nominal frequency of the system.

$$RoCof = \frac{d(\Delta f)}{dt} = \frac{f_0 (P_m - P_e)}{2HS} \quad (5)$$

III. METHOD

A. Test System

This study uses a multi-area AGC system. The AGC scheme is useful when the system load changes continuously [44]. Therefore, the generation is customized automatically to recover the frequency [45]. The five-area system in this study is shown in Fig. 1 because most of the research in the AGC field is concerned with the same two-area thermal system, and not much attention is paid to the different multi-area AGC systems [46]. In Fig. 2, the design of the five-area AGC system is modeled from the reference [47].

The transfer function of the governor shows (6).

$$G_g(s) = \frac{K_g}{T_g s + 1} \quad (6)$$

Meanwhile, the transfer function of the non-reheat turbine in (7) in (8) is the transfer function for rotating mass & load [48].

$$G_t(s) = \frac{K_t}{T_t s + 1} \quad (7)$$

$$G_p(s) = \frac{K_p}{T_p s + 1} \quad (8)$$

The five-area system gets the frequency deviation equation at (9) to (13) [49].

$$\Delta f_1(s) = \left[\frac{K_p}{T_p s + 1} \right] [\Delta P_m(s) - \Delta P_L(s) - \Delta P_{TL1}(s)] \quad (9)$$

$$\Delta f_2(s) = \left[\frac{K_p}{T_p s + 1} \right] [\Delta P_m(s) - \Delta P_L(s) - \Delta P_{TL2}(s)] \quad (10)$$

$$\Delta f_3(s) = \left[\frac{K_p}{T_p s + 1} \right] [\Delta P_m(s) - \Delta P_L(s) - \Delta P_{TL3}(s)] \quad (11)$$

$$\Delta f_4(s) = \left[\frac{K_p}{T_p s + 1} \right] [\Delta P_m(s) - \Delta P_L(s) - \Delta P_{TL4}(s)] \quad (12)$$

$$\Delta f_5(s) = \left[\frac{K_p}{T_p s + 1} \right] [\Delta P_m(s) - \Delta P_L(s) - \Delta P_{TL5}(s)] \quad (13)$$

Meanwhile, the tie-line power deviation equation points (14) to (18) [50].

$$\begin{aligned} \Delta P_{TL1}(s) = & \frac{2\pi T}{s} \Delta f_1(s) - \Delta f_2(s) + \frac{2\pi T}{s} \Delta f_1(s) - \Delta f_3(s) + \frac{2\pi T}{s} \Delta f_1(s) \\ & - \Delta f_4(s) + \frac{2\pi T}{s} \Delta f_1(s) - \Delta f_5(s) \end{aligned} \quad (14)$$

$$\begin{aligned} \Delta P_{TL2}(s) = & \frac{2\pi T}{s} \Delta f_2(s) - \Delta f_1(s) + \frac{2\pi T}{s} \Delta f_2(s) - \Delta f_3(s) + \frac{2\pi T}{s} \Delta f_2(s) \\ & - \Delta f_4(s) + \frac{2\pi T}{s} \Delta f_2(s) - \Delta f_5(s) \end{aligned} \quad (15)$$

$$\begin{aligned} \Delta P_{TL3}(s) = & \frac{2\pi T}{s} \Delta f_3(s) - \Delta f_1(s) + \frac{2\pi T}{s} \Delta f_3(s) - \Delta f_2(s) + \frac{2\pi T}{s} \Delta f_3(s) \\ & - \Delta f_4(s) + \frac{2\pi T}{s} \Delta f_3(s) - \Delta f_5(s) \end{aligned} \quad (16)$$

$$\begin{aligned} \Delta P_{TL4}(s) = & \frac{2\pi T}{s} \Delta f_4(s) - \Delta f_1(s) + \frac{2\pi T}{s} \Delta f_4(s) - \Delta f_2(s) + \frac{2\pi T}{s} \Delta f_4(s) \\ & - \Delta f_3(s) + \frac{2\pi T}{s} \Delta f_4(s) - \Delta f_5(s) \end{aligned} \quad (17)$$

$$\begin{aligned} \Delta P_{TL5}(s) = & \frac{2\pi T}{s} \Delta f_5(s) - \Delta f_1(s) + \frac{2\pi T}{s} \Delta f_5(s) - \Delta f_2(s) + \frac{2\pi T}{s} \Delta f_5(s) \\ & - \Delta f_3(s) + \frac{2\pi T}{s} \Delta f_5(s) - \Delta f_4(s) \end{aligned} \quad (18)$$

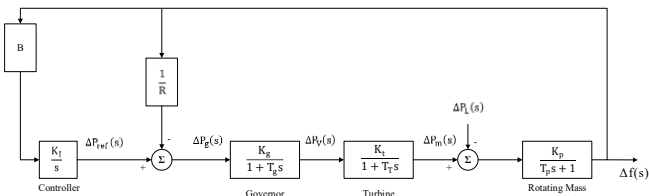


Fig. 2. Non-Reheat Thermal Generation System

B. PID-based BESS

The performance of energy storage devices can be determined by the energy produced and their energy density [51]. The use of energy storage can be distinguished by place and duration of use, as determined by the technology used [52]. Battery technology in energy storage devices can be distinguished based on energy density, round trip efficiency, lifetime, and environmental friendliness of the device [53].

One of the most important performance elements of energy storage devices is their service life, this has the greatest influence in terms of economic efficiency [54]. In addition, environmental friendliness is a major consideration because the device is not harmful to the environment and can be recycled [55].

Technically, BESS has proven to be able to provide frequency regulation [57]. BESS response times (in seconds) are much faster than conventional power plants (typically 3-5 seconds). Thus, the energy policy must have the technical capabilities of all types of assets including BESS to be used in frequency regulation [19]. Some examples of projects (BESS), Supercapacitor Energy Storage (SCES), Flywheel Energy Storage (FES), and Superconducting Magnetic Energy Storage (SMES) in the real world are shown in Table II. The projects mentioned are not meant for frequency setting. BESS projects in Japan and Ireland are used to reduce fluctuations in wind power generation [56].

TABLE II. REAL-WORLD ENERGY STORAGE FACILITIES AND THEIR APPLICATIONS [56]

Name/Location	Rating	Application
BES/Australia	30 MW/8 MWh	Fast frequency response
BES/USA	8 MW/2 MWh	Frequency regulation
BES/Germany	8.5 MW/8.5 MWh	Frequency control, spinning reserve
BES/Puerto Rico	20 MW/14 MWh	Frequency control, spinning reserve
BES/Japan	34 MW/244.8 MWh	Wind power fluctuation mitigation
BES/USA	10 MW/40 MWh	Spinning reserve, load leveling
BES/Ireland	2 MW/12 MWh	Wind power fluctuation mitigation
SCES/China	3 MW/17.2 kWh	Voltage sag mitigation
SCES/Spain	4 MW/5.6 kWh	Frequency stability
FES/USA	20 MW	Frequency regulation, power quality
FES/Japan	235 MVA	High power supply to nuclear fusion furnace
SMES/Japan	10 MW	System stability, power quality

The BESS model shows in Fig. 3. The main important thing is to examine postponing measurement, command, and converter in the model [58]. The BESS equation points to (19) [59].

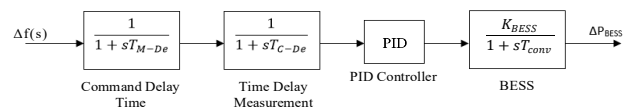


Fig. 3. BESS Model

$$G_{BESS}(s) = \frac{K_{BESS}}{T_{conv}s + 1} \quad (19)$$

Conventional PID control is appended to the designated BESS (20), used to prevent active power mismatches in energy storage systems [60].

$$PID\ Control = P \left(1 + I \frac{1}{s} + D \frac{N}{1 + N \frac{1}{s}} \right) \quad (20)$$

The determination of the PID parameter is carried out in several stages [61]. The first step is to determine the P parameter to reduce the maximum oscillation but produces continuous oscillations [62]. In the condition of the five-area AGC system with the addition of BESS, the undershoot value is greater than the overshoot value [63]. Therefore, after adding the P parameter, the undershoot value is greater than the overshoot value [64]. The second stage is to decrease the undershoot value by parameter I, causing the overshoot value to increase [65]. The addition of the PI parameter has resulted in good attenuation of fluctuations, characterized by overshoot and undershoot values that are smaller than the target operating frequency but have prolonged oscillations and exceed the target time to recover frequency [66]. Therefore, the last step is the addition of parameter D to dampen continuous oscillations [67]. If we look at the response generated by each PID parameter, parameter D gets the best response because it can dampen fluctuations without producing an impact [68]. However, because parameter D cannot stand alone, but must be paired with P [69]. This also affects parameter I, which must be paired with parameter P. Previously, the influence of the PI parameter can meet the overshoot and undershoot limits but cannot meet the time to recover frequency [70]. While the use of the PD parameter gets the opposite result, which can meet the time to recover frequency and cannot meet the target undershoot value. Therefore, the PID parameter is used to meet the target operating frequency [71].

C. Index Criterion

The objective function is determined in advance for the design of optimization techniques based on the desired specifications and constraints [72]. The objective function used to optimize the controller parameters is typically chosen based on performance criteria that are dependent on system response [73]. The desired specification in a time domain system is the value of overshoot, rise time, settling time, and steady-state error [74].

The Integral of Time multiplied Absolute Error (ITAE) is given in equation (21), the Integral of Time multiplied Squared Error (ITSE) is given in equation (22), the Integral of Absolute Error (IAE) is given in equation (23), and the Integral of Squared Error (ISE) is given in equation (24) [75].

$$ITAE = \int t|ACE|dt \quad (21)$$

$$ITSE = \int t\{ACE\}^2 dt \quad (22)$$

$$IAE = \int |ACE|dt \quad (23)$$

$$ISE = \int \{ACE\}^2 dt \quad (24)$$

Because the ISE criterion rejects major errors more than minor ones, it tends to eliminate major errors quickly while retaining minor errors for long periods of time [76]. This results in a fast response, but with a sufficiently large and low amplitude, causing unwanted oscillations [77]. Because the IAE criterion aggregates errors over time and does not weight any errors in the system response, the IAE tends to produce a slower response than the ISE criterion, but with fewer sustained oscillations [78]. The ITAE criterion incorporates errors that are multiplied by time over time, so the weight of the errors over time is much greater than the weight of the errors in the initial response [79]. The ITSE criteria provide a large controller output for abrupt changes in set-point, which are undesirable from the standpoint of controller design [80].

IV. RESULTS AND DISCUSSION

In this study, a five-area AGC system simulation is proposed to be carried out using MATLAB software. In the condition of the power plant, the thermal AGC interconnection of five areas experiences changes in the electrical load with dynamic disturbances, which increase frequency fluctuations. Therefore, the power frequency fluctuation was reduced by BESS, with the addition of a PID, which is used as the BESS control system to improve frequency stability better and faster. In other conditions, the addition of BESS requires costs for BESS purchases, installation, and so on. Therefore, to save costs on BESS installation, a study was conducted to install one BESS in a five-area AGC system, based on the location of the BESS installation area that received the best response to attenuation of frequency fluctuations. However, each region has a different frequency operating standard. Thus, to meet the frequency operating standards that have not been met by the addition of one BESS, a study was conducted on the number of BESS installations to reduce frequency fluctuations better than one BESS. Fig. 4 show the flowchart of the research procedure.

This research is carried out to improve the frequency stability of the multi-area AGC system, namely the non-reheat thermal five-area AGC system, for the result of Frequency Fluctuation Response of AGC can be seen in Fig. 5 and Fig. 6. Repairs are carried out by referring to the standard operating frequency set by ENTSO-E. There are four operating standards with two different maximum steady-state frequency deviation values, namely the GB, IRE, and NE standards working at ± 500 mHz. In comparison, the CE standard has a smaller value, which has a maximum steady-state frequency deviation value of ± 200 mHz. Therefore, the target for improving frequency stability is to get a maximum steady-state frequency deviation value of ± 200 mHz or ± 0.004 p.u.

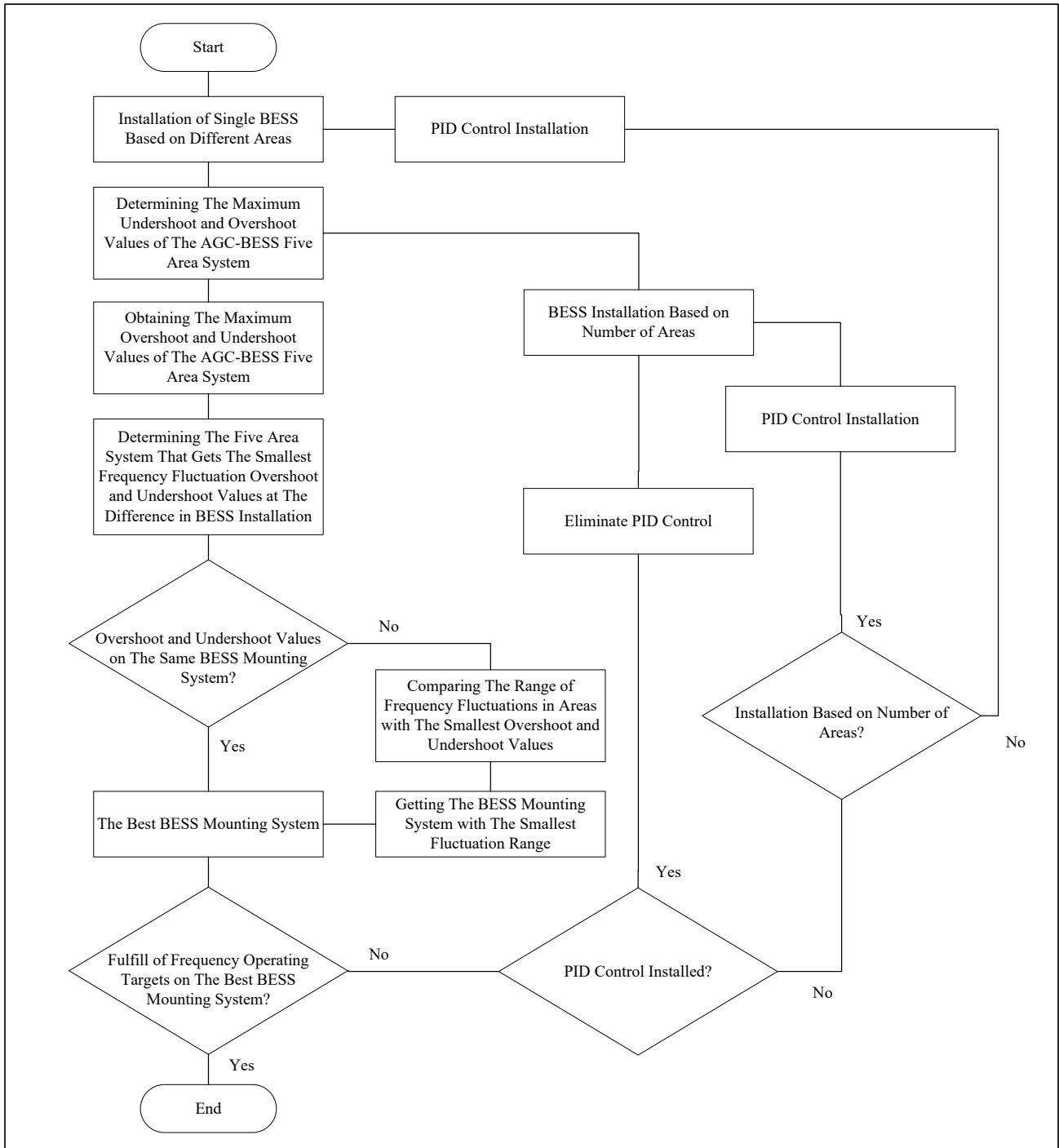


Fig. 4. Flowchart of the Paper

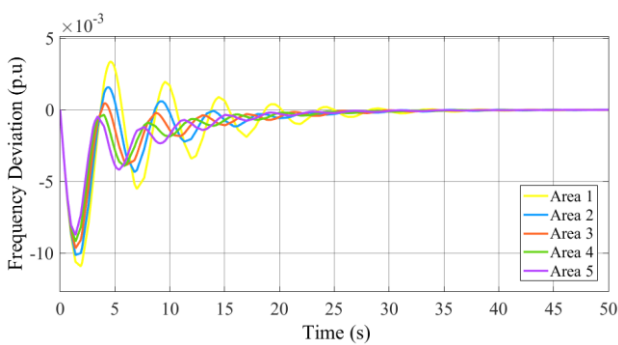


Fig. 5. Frequency Fluctuation Response of AGC Five Area System

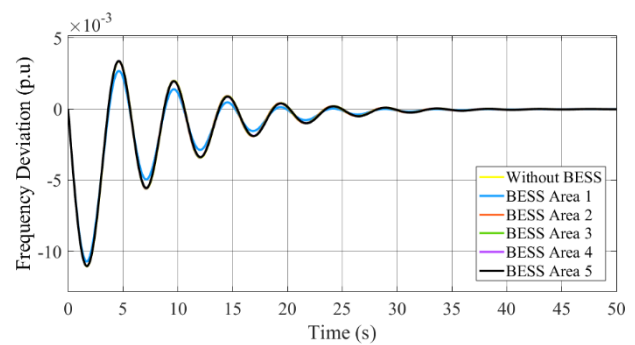


Fig. 6. Comparison of IRON Laying Responses to the Largest Frequency Fluctuations

The five-area AGC system gets area 1, as the area that gets the largest frequency fluctuation compared to other areas, as shown in Fig. 5. Installation of BESS to improve frequency stability in the area that has the largest frequency fluctuation, namely in area 1, which refers to Fig. 5. This is proven by the decrease in the value of frequency fluctuations after using BESS and compared to before using BESS, the installation of BESS area 1 can reduce the overshoot of maximum frequency fluctuations from other areas, reduce the overshoot of maximum frequency fluctuations by 20.565% and 2.014% in the undershoot value. Meanwhile, for the installation of BESS in area 5, the worst response in improving the frequency stability of the five-area AGC system shows that the maximum frequency fluctuation has increased after the installation of BESS, an increase in overshoot fluctuation of 0.296%, and an undershoot fluctuation of 1.007%. For the response of BESS PID in five-area can be seen in Fig. 7 to Fig. 11, and shown in Table III for detailed results features.

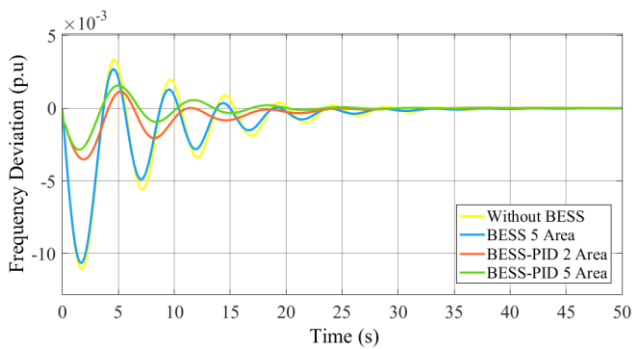


Fig. 7. Response of BESS PID Frequency Fluctuation in Area 1

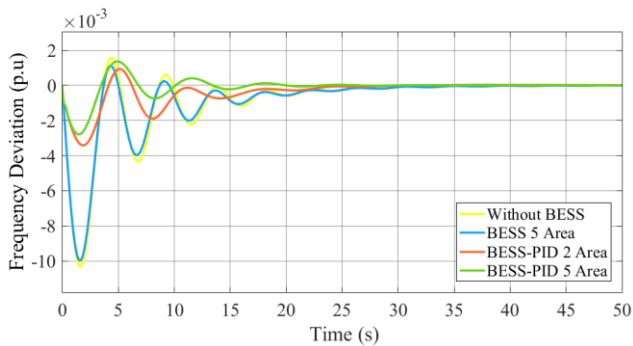


Fig. 8. Response of BESS PID Frequency Fluctuation in Area 2

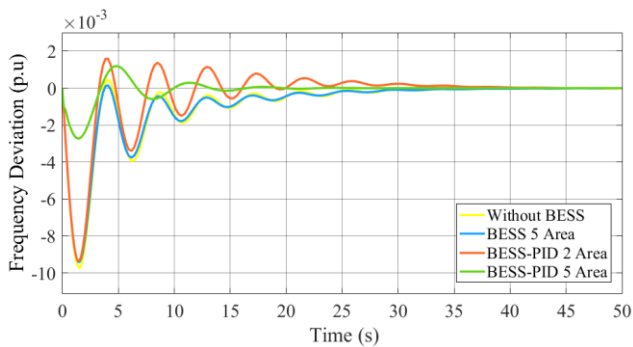


Fig. 9. Response of BESS PID Frequency Fluctuation in Area 3

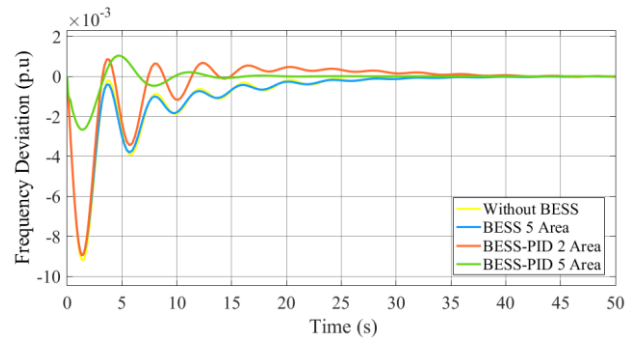


Fig. 10. Response of BESS PID Frequency Fluctuation in Area 4

Based on the data that has been obtained, the installation of 1 BESS area causes the system to get the largest overshoot value of $2.669e-3$ p.u (50.133 Hz). While the largest undershoot value is $1.070e-2$ p.u or the frequency becomes 49.465 Hz. Referring to Fig. 5, the installation of 5 BESS areas got a better response than 1 area in reducing frequency fluctuations. The maximum frequency overshoot value obtained was 50.134 Hz ($2.687e-3$ pu), and the maximum frequency undershoot value was 49.467 Hz ($1.065e-2$ pu). Although the difference in the response of the installation of 1 BESS area to 5 areas is very small, it can be concluded that the more BESS used, the better response to attenuation of frequency fluctuations.

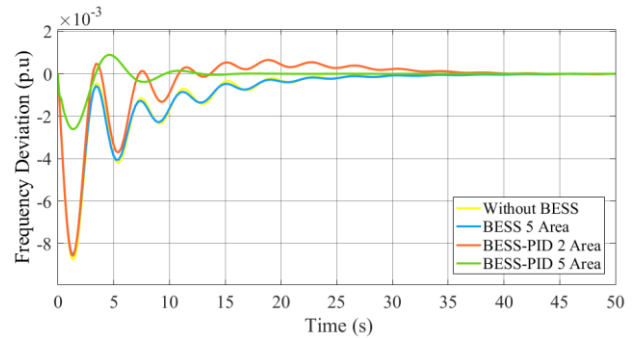


Fig. 11. Response of BESS PID Frequency Fluctuation in Area 5

The installation of 5 BESS areas causes the system to operate in a frequency range of 49.467 Hz to 50.134 Hz, obtaining an Integral of Squared Error (ISE) performance criterion of 0.269. This shows that the reduction of the undershoot of the largest frequency fluctuations must be made better because it has not reached the expected target. The smaller the ISE performance criteria value can eliminate fluctuations with a large peak value. Hence, to get better attenuation, use the PID control to set BESS. Referring to Fig. 7 to Fig. 11, the five-area AGC system with 5 BESS PID areas received a better response than the uncontrolled BESS, indicated by the achievement of improvement targets and meeting the standard operating frequencies of GB, IRE, NE, and CE. The use of 5 BESS PID areas gets an ISE performance criterion value of 0.021, causing the system to operate in the frequency range of 50.078 Hz to 49.857 Hz.

TABLE III. DETAILED FEATURES OF FIG 7-11

	Overshoot (p.u)	Undershoot (p.u)	Settling Time (s)
Δf_1	1.982e-3	1.128e-3	26.004
Δf_2	1.798e-3	9.070e-4	20.041
Δf_3	1.654e-3	7.365e-4	16.578
Δf_4	1.534e-3	5.993e-4	13.402
Δf_5	1.435e-3	4.899e-4	12.743

Each region has a different standard operating frequency in areas that use the standard operating frequencies of GB, IRE, and NE, which is the maximum steady-state frequency deviation value of ± 500 MHz. The installation of 2 BESS PID areas on the five-area AGC system can meet these operating standards because the system works in the frequency range of 49.531 Hz to 50.080 Hz. Fig. 10 shows the system response under 4 different criteria namely ITAE, ITSE, IAE and ISE. While Table IV shows the detailed features of Fig. 12.

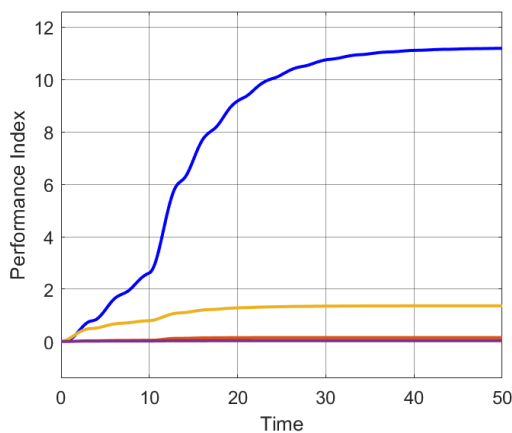


Fig. 12. Criterion Index Figure.

TABLE IV. DETAILED FEATURES OF FIG 12

Index	Value	Settling Time (s)
ITAE	11.193	35.538
ITSE	0.151	22.712
IAE	1.362	26.869
ISE	0.029	17.627

From all the results it is found that the system with BESS has a lower frequency overshoot compared to the system without BESS. This could have happened because BESS released and stored energy faster than the ramp-up of the generator. Hence, in the first swings when the load disturbance occurs, BESS provides electricity to the grid. Resulting in reducing the overshoot of the frequency. BESS could provide inertia control without getting any rotating machine when the disturbance occurs (it is called virtual inertia support). After 5 seconds, the power plant starts to ramp up the generating capacity to provide electricity as requested by the grid.

It is also found that adding additional controllers such as the PID controller at BESS could also enhance the frequency response of the generator. This could have happened because the PID controller gave more details control signals to BESS rather than the gain controller only. If the control signals are more detailed, the BESS could provide electricity faster. In addition, the BESS could also provide more detailed power to

the system when the PID controller is added as the additional controller.

V. CONCLUSIONS

This study improves the frequency stability of the AGC for multi-area non-reheat thermal power, using BESS and PID control. The use of BESS in multi-area AGC can smooth and slightly dampen the frequency oscillation waves. The use of BESS with PID control can reduce frequency fluctuations better. Installation of BESS is recommended in areas that have the greatest frequency fluctuations because it can reduce frequency fluctuations in multi-area systems. The more areas BESS has installed, the better it can dampen frequency fluctuations. For further research, adding non-inertia power plants such as PV and wind power systems can be considered to investigate how the BESS could maintain the frequency of the system under low inertia grid conditions.

ABBREVIATION

α	Area synchronization parameters
B	Area frequency response characteristics
D	Derivative parameters
F	AGC five area system frequency
I	Integral Parameters
K_{BESS}	BESS coefficient
K_g	Steam governor coefficient
K_i	AGC five area system integral control parameter
K_p	Load coefficient
K_t	Steam turbine coefficient
L	Load on area
N	Filter coefficient
P	Proportional Parameters
R	Governor speed regulation
T	Synchronization coefficient
$T_{\text{C-De}}$	Order delay time
T_{conv}	Converter time
T_g	Time constant steam governor
$T_{\text{M-De}}$	Measurement delay time
T_p	Time constant load
T_t	Time constant steam turbine

APPENDIX

Power rating: Area 1=2000 MW, Area 2=4000 MW, Area 3=8000 MW, Area 4=10000 MW, Area 5=12000 MW; $B_1=B_2=B_3=B_4=B_5=16$ p.u. MW/Hz; $K_{i1}=K_{i2}=K_{i3}=K_{i4}=K_{i5}=0,3$; $a_{12}=-0,5$, $a_{13}=-0,25$, $a_{14}=-0,2$, $a_{15}=-0,167$, $a_{23}=-0,5$, $a_{24}=-0,4$, $a_{25}=-0,333$, $a_{34}=-0,8$, $a_{35}=-0,667$, $a_{45}=-0,833$; $R_1=0,04$ Hz/p.u. MW, $R_2=0,033$ Hz/p.u. MW, $R_3=0,028$ Hz/p.u. MW, $R_4=0,025$ Hz/p.u. MW, $R_5=0,022$ Hz/p.u. MW; $T=0,544$; $T_t=0,3$ s; $T_g=0,8$ s; $T_p=20$ s; $K_p=1$ Hz/p.u. MW; $K_g=1$ Hz/p.u. MW; $K_t=1$ Hz/p.u. MW; $K_{\text{BESS}}=1$; $T_{\text{conv}}=0,1$ s; $T_{\text{C-De}}=0,01$ s; $T_{\text{M-De}}=0,1$ s; $P=10$; $I=4$; $D=5$; $N=100$; $F=50$ Hz; $L=0,2$ p.u.

ACKNOWLEDGMENT

The corresponding author would like to thanks to Universitas Airlangga for funding this research through

“Penelitian Dosen Pemula” grant (grant number: 416/UN3.1.17/PT/2023).

REFERENCES

- [1] CH. N. S. Kalyan *et al.*, “Comparative Performance Assessment of Different Energy Storage Devices in Combined LFC and AVR Analysis of Multi-Area Power System,” *Energies (Basel)*, vol. 15, no. 2, p. 629, Jan. 2022, doi: 10.3390/en15020629.
- [2] Y. Shen, W. Yao, J. Wen, H. He and L. Jiang, “Resilient Wide-Area Damping Control Using GrHDP to Tolerate Communication Failures,” in *IEEE Transactions on Smart Grid*, vol. 10, no. 3, pp. 2547-2557, May 2019, doi: 10.1109/TSG.2018.2803822.
- [3] V. Vittal, J. D. McCalley, P. M. Anderson, and A. A. Fouad, *Power system control and stability*. John Wiley & Sons, 2019.
- [4] Y. Arya, “AGC performance enrichment of multi-source hydrothermal gas power systems using new optimized FOPID controller and redox flow batteries,” *Energy*, vol. 127, pp. 704–715, 2017, doi: <https://doi.org/10.1016/j.energy.2017.03.129>.
- [5] K. Jagatheesan, B. Anand, and S. Samanta, “Flower Pollination Algorithm Tuned PID Controller for Multi-source Interconnected Multi-area Power System,” *Applications of Flower Pollination Algorithm and its Variants*, pp. 221-239, 2021.
- [6] M. A. Kamarposhti, H. Shokouhandeh, M. Alipur, I. Colak, H. Zare, and K. Eguchi, “Optimal Designing of Fuzzy-PID Controller in the Load-Frequency Control Loop of Hydro-Thermal Power System Connected to Wind Farm by HVDC Lines,” *IEEE Access*, vol. 10, pp. 63812–63822, 2022.
- [7] R. K. Sahu, S. Panda, and S. Padhan, “A hybrid firefly algorithm and pattern search technique for automatic generation control of multi area power systems,” *International Journal of Electrical Power & Energy Systems*, vol. 64, pp. 9–23, 2015.
- [8] A. Dhamanda and A. K. Bhardwaj, “Multi Area AGC Problem of TGU Solved Through GA (Using Tuning of PID) Controller,” *International Journal of Advancements in Technology*, vol. 9, no. 207, pp. 1-13, 2018.
- [9] X. Liu, X. Zhan, and D. Qian, “Load frequency control considering generation rate constraints,” in *2010 8th World Congress on Intelligent Control and Automation*, pp. 1398–1401, 2010.
- [10] X. Zhang, T. Tan, B. Zhou, T. Yu, B. Yang, and X. Huang, “Adaptive distributed auction-based algorithm for optimal mileage based AGC dispatch with high participation of renewable energy,” *International Journal of Electrical Power & Energy Systems*, vol. 124, p. 106371, 2021.
- [11] J. R. Nayak, B. Shaw, B. K. Sahu, and K. A. Naidu, “Application of optimized adaptive crow search algorithm based two degree of freedom optimal fuzzy PID controller for AGC system,” *Engineering Science and Technology, an International Journal*, vol. 32, p. 101061, 2022.
- [12] D. Guha, P. K. Roy, and S. Banerjee, “Equilibrium optimizer-tuned cascade fractional-order 3DOF-PID controller in load frequency control of power system having renewable energy resource integrated,” *International Transactions on Electrical Energy Systems*, vol. 31, no. 1, p. e12702, 2021.
- [13] M. Sterner and I. Stadler, *Handbook of energy storage: Demand, technologies, integration*. Springer, 2019.
- [14] S. Gurung, S. Naetiladnanon, and A. Sangswang, “Coordination of power-system stabilizers and battery energy-storage system controllers to improve probabilistic small-signal stability considering integration of renewable-energy resources,” *Applied Sciences*, vol. 9, no. 6, p. 1109, 2019.
- [15] K. M. Kotb, M. F. Elmorshedy, H. S. Salama, and A. Dán, “Enriching the stability of solar/wind DC microgrids using battery and superconducting magnetic energy storage based fuzzy logic control,” *Journal of Energy Storage*, vol. 45, p. 103751, Jan. 2022, doi: 10.1016/j.est.2021.103751.
- [16] A. Naderipour, A. R. Ramtin, A. Abdullah, M. H. Marzbali, S. A. Nowdeh, and H. Kamyab, “Hybrid energy system optimization with battery storage for remote area application considering loss of energy probability and economic analysis,” *Energy*, vol. 239, p. 122303, 2021.
- [17] P. Xie, J. Zhu, and P. Xuan, “Optimal controller design for AGC with battery energy storage using bacteria foraging algorithm,” *2017 IEEE Power & Energy Society General Meeting*, pp. 1-1, 2017, doi: 10.1109/PESGM.2017.8274506.
- [18] D. Kottick, M. Blau, and D. Edelstein, “Battery energy storage for frequency regulation in an island power system,” *IEEE transactions on energy conversion*, vol. 8, no. 3, pp. 455–459, 1993.
- [19] D. K. Kim, S. Yoneoka, A. Z. Banatwala, Y.-T. Kim, and K. Y. Nam, “Handbook on battery energy storage system,” *Asian Development Bank: Manila, Philippines*, 2018.
- [20] H. Setiadi *et al.*, “Influence of Adding BESS as Ancillary Controller of Wind Power Plant on Low Frequency Oscillation,” *International Journal of Intelligent Engineering and Systems*, vol. 14, no. 5, pp. 188–198, 2021.
- [21] S. Chatterjee, M. A. Islam, M. K. Chileshe, and A. A. I. Osman, “Automatic Generation Control using Whale Optimization Algorithm tuned PID Controller,” *Image Processing in Renewable: Energy Resources Opportunities and Challenges*, vol. 1, p. 58, 2022.
- [22] A. M. Allam, A. S. Ibrahim, and E. Nabil, “Single loop PID controller design based on optimization algorithms for parallelly connected dc-dc converters,” in *Journal of Physics: Conference Series*, vol. 2128, p. 012027, 2021.
- [23] N. Razmjoo, Z. Vahedi, V. v. Estrela, R. Padilha, and A. C. B. Monteiro, “Speed Control of a DC Motor Using PID Controller Based on Improved Whale Optimization Algorithm,” *Metaheuristics and Optimization in Computer and Electrical Engineering*, pp. 153–167, 2021.
- [24] J.-P. Lee and H.-G. Kim, “Application of FESS controller for load frequency control,” in *Journal of international Conference on Electrical Machines and Systems, Journal of International Conference on Electrical Machines and Systems*, pp. 361–366, 2013.
- [25] K. H. Ang, G. Chong, and Y. Li, “PID control system analysis, design, and technology,” *IEEE transactions on control systems technology*, vol. 13, no. 4, pp. 559–576, 2005.
- [26] M. Abdillah, “Adaptive Hybrid Fuzzy PI-LQR Optimal Control using Artificial Immune System via Clonal Selection for Two-Area Load Frequency Control,” *International Journal on Electrical Engineering and Informatics*, vol. 12, no. 3, pp. 667–685, Sep. 2020, doi: 10.15676/ijeii.2020.12.3.14.
- [27] K. Arora, A. Kumar, V. K. Kamboj, D. Prashar, B. Shrestha, and G. P. Joshi, “Impact of renewable energy sources into multi area multi-source load frequency control of interrelated power system,” *Mathematics*, vol. 9, no. 2, p. 186, 2021.
- [28] M. MV and V. V, “Model-predictive control-based hybrid optimized load frequency control of multi-area power systems,” *IET Generation, Transmission & Distribution*, vol. 15, no. 9, pp. 1521–1537, 2021.
- [29] T. Kerdphol, M. Watanabe, K. Hongesombut, and Y. Mitani, “Self-adaptive virtual inertia control-based fuzzy logic to improve frequency stability of microgrid with high renewable penetration,” *IEEE Access*, vol. 7, pp. 76071–76083, 2019.
- [30] N. Wang *et al.*, “Load-frequency control of multi-area power system based on the improved weighted fruit fly optimization algorithm,” *Energies (Basel)*, vol. 13, no. 2, p. 437, 2020.
- [31] T. Kerdphol, F. S. Rahman, M. Watanabe, and Y. Mitani, *Virtual Inertia Synthesis and Control*, 1st ed. Cham: Springer International Publishing, 2021. doi: 10.1007/978-3-030-57961-6.
- [32] V. Soni, G. Parmar, and M. Kumar, “A hybrid grey wolf optimisation and pattern search algorithm for automatic generation control of multi-area interconnected power systems,” *International Journal of Advanced Intelligence Paradigms*, vol. 18, no. 3, pp. 265–293, 2021.
- [33] T. Kerdphol, F. S. Rahman, M. Watanabe, and Y. Mitani, “Robust virtual inertia control of a low inertia microgrid considering frequency measurement effects,” *IEEE Access*, vol. 7, pp. 57550–57560, 2019.
- [34] H. Saadat, “Power System Analysis, (2nd),” *McGraw-Hill Higher Education*, 2009.
- [35] T. Kerdphol, F. S. Rahman, Y. Mitani, M. Watanabe, and S. K. Küfeoglu, “Robust virtual inertia control of an islanded microgrid considering high penetration of renewable energy,” *IEEE Access*, vol. 6, pp. 625–636, 2017.
- [36] J. Gouveia, C. L. Moreira, and J. A. P. Lopes, “Rule-based adaptive control strategy for grid-forming inverters in islanded power systems for improving frequency stability,” *Electric Power Systems Research*,

- vol. 197, p. 107339, 2021, doi: <https://doi.org/10.1016/j.eprs.2021.107339>.
- [37] M. Eskandari, A. V. Savkin, and J. Fletcher, "A Deep Reinforcement Learning-based Intelligent Grid-Forming Inverter for Inertia Synthesis by Impedance Emulation," *IEEE Transactions on Power Systems*, 2023.
- [38] S. K. Singh, R. Singh, H. Ashfaq, and R. Kumar, "Virtual inertia emulation of inverter interfaced distributed generation (IIDG) for dynamic frequency stability & Damping enhancement through BFOA tuned optimal controller," *Arabian Journal for Science and Engineering*, vol. 47, no. 3, pp. 3293–3310, 2022.
- [39] A. Saleh, W. A. Omran, H. M. Hasanien, M. Tostado-Véliz, A. Alkuhayli, and F. Jurado, "Manta Ray Foraging Optimization for the Virtual Inertia Control of Islanded Microgrids Including Renewable Energy Sources," *Sustainability*, vol. 14, no. 7, p. 4189, 2022.
- [40] P. Kundur, *Power System Stability and Control*. New York: McGraw-Hill, 1994.
- [41] E. Rokrok, T. Qoria, A. Bruyere, B. Francois, and X. Guillaud, "Classification and dynamic assessment of droop-based grid-forming control schemes: Application in HVDC systems," *Electric Power Systems Research*, vol. 189, p. 106765, 2020.
- [42] H. Bevrani, B. François, and T. Ise, *Microgrid dynamics and control*. John Wiley & Sons, 2017.
- [43] H. Bevrani, *Robust power system frequency control*, vol. 4. Springer, 2014.
- [44] D. H. Tungadio and Y. Sun, "Load frequency controllers considering renewable energy integration in power system," *Energy Reports*, vol. 5, pp. 436–453, 2019.
- [45] H. Saadat, *Power System Analysis McGraw-Hill Series in Electrical Computer Engineering*.
- [46] L. C. Saikia, J. Nanda, and S. Mishra, "Performance comparison of several classical controllers in AGC for multi-area interconnected thermal system," *International Journal of Electrical Power & Energy Systems*, vol. 33, no. 3, pp. 394–401, 2011.
- [47] S. Padhy, S. Panda, and S. Mahapatra, "A modified GWO technique based cascade PI-PD controller for AGC of power systems in presence of plug in electric vehicles," *Engineering Science and Technology, an International Journal*, vol. 20, no. 2, pp. 427–442, 2017.
- [48] S. Oshnoei, A. Oshnoei, A. Mosallanejad, and F. Haghjoo, "Novel load frequency control scheme for an interconnected two-area power system including wind turbine generation and redox flow battery," *International Journal of Electrical Power & Energy Systems*, vol. 130, p. 107033, 2021.
- [49] K. I. Annaporani, V. Rajaguru, S. A. Padmanabhan, K. M. Kumar, and S. Venkatachalam, "Fuzzy logic-based integral controller for load frequency control in an isolated micro-grid with superconducting magnetic energy storage unit," *Materialstoday Proceedings*, vol. 58, pp. 244–250, 2022, doi: 10.1016/j.matpr.2022.02.103.
- [50] M. A. Sobhy, A. Y. Abdelaziz, H. M. Hasanien, and M. Ezzat, "Marine predators algorithm for load frequency control of modern interconnected power systems including renewable energy sources and energy storage units," *Ain Shams Engineering Journal*, vol. 12, no. 4, pp. 3843–3857, 2021.
- [51] H. Setiadi, N. Mithulananthan, R. Shah, K. Y. Lee, and A. U. Krismanto, "Resilient wide-area multi-mode controller design based on Bat algorithm for power systems with renewable power generation and battery energy storage systems," *IET Generation, Transmission & Distribution*, vol. 13, no. 10, pp. 1884–1894, 2019.
- [52] H. Setiadi, A. Swandaru, D. A. Asfani, T. H. Nasution, M. Abdillah, and A. U. Krismanto, "Coordinated Design of DIPSS and CES Using MDEA for Stability Enhancement: Jawa-Bali Indonesian Power Grid Study Case," *International Journal of Intelligent Engineering and Systems*, vol. 15, no. 1, pp. 251–261, 2022.
- [53] H. Mohammadi Moghadam, A. Mohammadzadeh, R. Hadjiaghaie Vafaie, J. Tavoosi, and M.-H. Khooban, "A type-2 fuzzy control for active/reactive power control and energy storage management," *Transactions of the Institute of Measurement and Control*, vol. 44, no. 5, pp. 1014–1028, 2022.
- [54] H. Zhang *et al.*, "Design and control of a new power conditioning system based on superconducting magnetic energy storage," *J Energy Storage*, vol. 51, p. 104359, Jul. 2022, doi: 10.1016/j.est.2022.104359.
- [55] N. Mughees, M. H. Jaffery, and M. Jawad, "A new predictive control strategy for improving operating performance of a permanent magnet synchronous generator-based wind energy and superconducting magnetic energy storage hybrid system integrated with grid," *Journal of Energy Storage*, vol. 55, p. 105515, 2022.
- [56] U. Akram, M. Nadarajah, R. Shah, and F. Milano, "A review on rapid responsive energy storage technologies for frequency regulation in modern power systems," *Renewable and Sustainable Energy Reviews*, vol. 120, p. 109626, 2020.
- [57] T. A. Nugroho, R. S. Wijanarko, and H. Setiadi, "Coordination of blade pitch controller and battery energy storage using firefly algorithm for frequency stabilization in wind power systems," *TELKOMNIKA (Telecommunication Computing Electronics and Control)*, vol. 17, no. 2, pp. 1014–1022, 2019.
- [58] M. Babaei, A. Abazari, and S. M. Muyeen, "Coordination between demand response programming and learning-based FOPID controller for alleviation of frequency excursion of hybrid microgrid," *Energies (Basel)*, vol. 13, no. 2, p. 442, 2020.
- [59] P. García-Triviño, R. Sarrias-Mena, C. A. García-Vázquez, S. Leva, and L. M. Fernández-Ramírez, "Optimal online battery power control of grid-connected energy-stored quasi-impedance source inverter with PV system," *Applied Energy*, vol. 329, p. 120286, 2023.
- [60] S. Priyadarshani, K. R. Subhashini, and J. K. Satapathy, "Pathfinder algorithm optimized fractional order tilt-integral-derivative (FOTID) controller for automatic generation control of multi-source power system," *Microsystem Technologies*, vol. 27, no. 1, pp. 23–35, 2021.
- [61] A. Baciu and C. Lazar, "Iterative Feedback Tuning of Model-Free Intelligent PID Controllers," in *Actuators*, p. 56, 2023.
- [62] B. Guo, Z. Zhuang, J.-S. Pan, and S.-C. Chu, "Optimal design and simulation for PID controller using Fractional-Order Fish Migration Optimization algorithm," *IEEE Access*, vol. 9, pp. 8808–8819, 2021.
- [63] A. M. Abdel-hamed, A. Y. Abdelaziz, and A. El-Shahat, "Design of a 2DOF-PID Control Scheme for Frequency/Power Regulation in a Two-Area Power System Using Dragonfly Algorithm with Integral-Based Weighted Goal Objective," *Energies (Basel)*, vol. 16, no. 1, p. 486, 2023.
- [64] M. Praharaj, D. Sain, and B. M. Mohan, "Development, experimental validation, and comparison of interval type-2 Mamdani fuzzy PID controllers with different footprints of uncertainty," *Information Sciences*, vol. 601, pp. 374–402, 2022.
- [65] M. Das, M. Catalkaya, O. E. Akay, and E. K. Akpınar, "Impacts of use PID control and artificial intelligence methods for solar air heater energy performance," *Journal of Building Engineering*, vol. 65, p. 105809, 2023.
- [66] D. Ertekin, K. Bulut, H. Tekin, and G. Moschopoulos, "A design for switched capacitor and single-switch DC–DC boost converter by a small signal-based PI controller," *International Journal of Circuit Theory and Applications*, vol. 50, no. 5, pp. 1620–1651, 2022.
- [67] S. Tufenkci, B. B. Alagoz, G. Kavuran, C. Yeroglu, N. Herencsar, and S. Mahata, "A theoretical demonstration for reinforcement learning of PI control dynamics for optimal speed control of DC motors by using Twin Delay Deep Deterministic Policy Gradient Algorithm," *Expert Systems with Applications*, vol. 213, p. 119192, 2023.
- [68] A. Mahapatro, P. R. Dhal, D. R. Parhi, M. K. Muni, C. Sahu, and S. K. Patra, "Towards stabilization and navigational analysis of humanoids in complex arena using a hybridized fuzzy embedded PID controller approach," *Expert Systems with Applications*, vol. 213, p. 119251, 2023.
- [69] R. El-Sehiemy, A. Shaheen, A. Ginidi, and S. F. Al-Gahtani, "Proportional-Integral-Derivative Controller Based-Artificial Rabbits Algorithm for Load Frequency Control in Multi-Area Power Systems," *Fractal and Fractional*, vol. 7, no. 1, p. 97, 2023.
- [70] E. S. Ghith and F. A. A. Tolba, "Tuning PID Controllers Based on Hybrid Arithmetic Optimization Algorithm and Artificial Gorilla Troop Optimization for Micro-Robotics Systems," in *IEEE Access*, vol. 11, pp. 27138–27154, 2023, doi: 10.1109/ACCESS.2023.3258187.
- [71] C. Lu, R. Tang, Y. Chen, and C. Li, "Robust tilt-integral-derivative controller synthesis for first-order plus time delay and higher-order systems," *International Journal of Robust and Nonlinear Control*, vol. 33, no. 3, pp. 1566–1592, 2023.

- [72] O. Gonzales-Zurita, O. L. Andino, J.-M. Clairand, and G. Escrivá-Escrivá, "PSO Tuning of a Second-Order Sliding Mode Controller for Adjusting Active Standard Power Levels for Smart Inverter Applications," *IEEE Trans Smart Grid*, 2023.
- [73] S. Gupta *et al.*, "Metaheuristic Optimization Techniques Used in Controlling of an Active Magnetic Bearing System for High-Speed Machining Application," *IEEE Access*, vol. 11, pp. 12100–12118, 2023.
- [74] Y. Zhi, W. Weiqing, C. Jing, and N. Razmjooy, "Interval linear quadratic regulator and its application for speed control of DC motor in the presence of uncertainties," *ISA Trans*, vol. 125, pp. 252–259, Jun. 2022, doi: 10.1016/j.isatra.2021.07.004.
- [75] H. Setiadi *et al.*, "Multi-Mode Damping Control Approach for the Optimal Resilience of Renewable-Rich Power Systems," *Energies (Basel)*, vol. 15, no. 9, p. 2972, 2022.
- [76] R. Kannan and V. Sundharajan, "A novel MPPT controller based PEMFC system for electric vehicle applications with interleaved SEPIC converter," *International Journal of Hydrogen Energy*, 2023.
- [77] D. Baidya, S. Dhopte, and M. Bhattacharjee, "Sensing System Assisted Novel PID Controller for Efficient Speed Control of DC Motors in Electric Vehicles," in *IEEE Sensors Letters*, vol. 7, no. 1, pp. 1–4, Jan. 2023, doi: 10.1109/LSENS.2023.3234400.
- [78] R. Saini, G. Parmar, and R. Gupta, "An enhanced hybrid stochastic fractal search FOPID for speed control of DC motor," in *Fractional Order Systems and Applications in Engineering*, pp. 51–67, 2023.
- [79] M. A. Abdullah, A. Q. Al-Shetwi, M. Mansor, M. A. Hannan, C. W. Tan, and A. H. M. Yatim, "Linear quadratic regulator controllers for regulation of the dc-bus voltage in a hybrid energy system: Modeling, design and experimental validation," *Sustainable Energy Technologies and Assessments*, vol. 50, p. 101880, Mar. 2022, doi: 10.1016/j.seta.2021.101880.
- [80] A. A. Hossam-Eldin, E. Negm, M. Ragab, and K. M. AboRas, "A maiden robust FPIDD2 regulator for frequency-voltage enhancement in a hybrid interconnected power system using Gradient-Based Optimizer," *Alexandria Engineering Journal*, vol. 65, pp. 103–118, 2023.